AGU PUBLICATIONS

Geophysical Research Letters

RESEARCH LETTER
10.1002/2015GL065879

Positive trends in Southern Hemisphere carbonyl sulfide

Stefanie Kremser[1], **Nicholas B. Jones**[2], **Mathias Palm**[3], **Bernard Lejeune**[4], **Yuting Wang**[3], **Dan Smale**[5], **and Nicholas M. Deutscher**[2]

[1]Bodeker Scientific, Alexandra, New Zealand, [2]School of Chemistry, University of Wollongong, Wollongong, New South Wales, Australia, [3]Department of Physics, University of Bremen, Bremen, Germany, [4]Institute of Astrophysics and Geophysics, University of Liège, Liège, Belgium, [5]NIWA Lauder, Lauder, New Zealand

Key Points:
- First observed positive trend in OCS in the Southern Hemisphere
- Observed trends indicate imbalanced OCS budget
- Temporal structure of trend is similar across middle- and high-latitude sites

Correspondence to:
S. Kremser,
stefanie@bodekerscientific.com

Citation:
Kremser, S., N. B. Jones, M. Palm, B. Lejeune, Y. Wang, D. Smale, and N. M. Deutscher (2015), Positive trends in Southern Hemisphere carbonyl sulfide, *Geophys. Res. Lett.*, *42*, 9473–9480, doi:10.1002/2015GL065879.

Received 20 AUG 2015
Accepted 16 OCT 2015
Accepted article online 21 OCT 2015
Published online 6 NOV 2015

Abstract Transport of carbonyl sulfide (OCS) from the troposphere to the stratosphere contributes sulfur to the stratospheric aerosol layer, which reflects incoming short-wave solar radiation, cooling the climate system. Previous analyses of OCS observations have shown no significant trend, suggesting that OCS is unlikely to be a major contributor to the reported increases in stratospheric aerosol loading and indicating a balanced OCS budget. Here we present analyses of ground-based Fourier transform spectrometer measurements of OCS at three Southern Hemisphere sites spanning 34.45°S to 77.80°S. At all three sites statistically significant positive trends are seen from 2001 to 2014 with an observed overall trend in total column OCS at Wollongong of 0.73 ± 0.03%/yr, at Lauder of 0.43 ± 0.02%/yr, and at Arrival Heights of 0.45 ± 0.05%/yr. These observed trends in OCS imply that the OCS budget is not balanced and could contribute to constraints on current estimates of sources and sinks.

1. Introduction

Carbonyl sulfide (OCS) is the longest-lived reduced sulfur gas in the atmosphere. The primary source of OCS is the ocean, which is both a direct source (through OCS emission) and an indirect source (due to oxidation of carbon disulfide, CS_2, and dimethyl sulfide) [*Kettle et al.*, 2002]. Other natural sources of OCS include volcanic outgassing and direct fluxes from wetland regions [*Kettle et al.*, 2002; *Kuai et al.*, 2014]. The removal of OCS from the atmosphere is dominated by soil and vegetation uptake, with minor contributions from reactions with the hydroxyl radical [*Kettle et al.*, 2002]. Small anthropogenic sources of OCS are coal combustion, biomass burning, and aluminum production [*Watts*, 2000]. A dominant indirect source results from CS_2 emissions from the rayon industry [*Campbell et al.*, 2015]. With a tropospheric lifetime of ~2–7 years [*Blake et al.*, 2004], OCS is sufficiently long-lived in the troposphere that it is transported into the stratosphere where it is photooxidized to form sulfate particles [*Sheng et al.*, 2015]. Previous studies suggested that OCS is a dominant contributor to the stratospheric aerosol layer during volcanically quiescent periods [*Crutzen*, 1976; *Pitari et al.*, 2002]. This finding is corroborated by a recent model-based study that indicates that although 90% of the OCS transported into the stratosphere returns unprocessed to the troposphere, the remaining OCS contributes ~56% to the stratospheric aerosol burden [*Sheng et al.*, 2015]. There has been some debate, however, on the magnitude of the OCS flux to the stratosphere and on the relative contribution of OCS to the stratospheric aerosol loading [*Brühl et al.*, 2012; *Chin and Davis*, 1995; *Myhre et al.*, 2004]. While many surface flask measurements of OCS were made from 2000 to 2006 [*Montzka et al.*, 2007], no significant trend was found over the Southern Hemisphere during this period, corroborating results from other studies [*Coffey and Hannigan*, 2010; *Griffith et al.*, 1998; *Rinsland et al.*, 2008]. These results, together with a study by *Sturges et al.* [2001] that demonstrated that OCS has changed little over the last 20 years of the twentieth century, suggest that it is unlikely that OCS is a major contributor to the increases in stratospheric aerosol loading that were reported by *Hofmann and Deshler* [1990]. More recently, ground-based lidar measurements have been used to infer a trend in stratospheric aerosol of 4 to 7%/yr, depending on location, since 2000 [e.g., *Hofmann et al.*, 2009]. The causes for those increases remain unclear and subject to debate, but potential candidates include increased coal combustion over China [*Hofmann et al.*, 2009] and small volcanic eruptions [*Vernier et al.*, 2011]. Furthermore, the absence of a significant trend in OCS observations indicates a balanced OCS budget for the observation period, an assumption used by model studies using OCS to infer additional information about the carbon cycle processes [e.g., *Berry et al.*, 2013]. However, estimates of OCS sources and sinks differ [*Campbell et al*., 2008; *Sandoval-Soto et al*., 2005; *Suntharalingam et al*., 2008], and therefore, large uncertainties in the OCS budget remain [*Kettle et al*., 2002; *Montzka et al*., 2007] and a debate whether or not the OCS budget is balance remains.

This paper presents the first analysis of long-term trends in total columns of OCS, as well as partial columns for the troposphere and stratosphere in the Southern Hemisphere. Retrieving tropospheric and stratospheric columns permits disaggregation of total column OCS changes into tropospheric and stratospheric contributions. The results presented here show a significant positive trend over the 2001 to 2014 period that was not previously observed in the Southern Hemisphere.

2. Method

2.1. Measurements

Ground-based Fourier transform spectrometer (FTS) measurements of OCS from 2001 to 2014 made at three different sites, representing diverse environments, in the Southern Hemisphere, viz., Wollongong, Australia (34.45°S, 150.88°E); Lauder, New Zealand (45.04°S, 169.68°E); and Arrival Heights, Antarctica (77.80°S, 166.67°E), are analyzed. OCS total and partial columns were derived from solar infrared spectra recorded by a Bruker 120HR at Lauder [*Jones et al*., 2009; *Zeng et al*., 2012], a Bruker 120M at Arrival Heights [*Wood et al*., 2002], and a Bomem DA8 from 2001 to August 2007 and a Bruker 125HR from August 2007 to 2014 at Wollongong [*Griffith et al*., 1998; *Kohlhepp et al*., 2012; *Paton-Walsh et al*., 2004]. To ensure that differences in OCS behavior across the three sites are unaffected by the configuration of the retrieval, the same retrieval settings were used at all three sites, i.e., fitting four microwindows covering the p19 (2053.98–2054.24 cm^{-1}), p25 (2051.18–2051.48 cm^{-1}), p28 (2049.75–2050.12 cm^{-1}), and p32 (2047.78–2048.22 cm^{-1}) lines of the OCS $\nu 3$ band. The interfering gases are carbon monoxide (CO), carbon dioxide (CO_2), water vapor, and ozone. The nonlinear fitting algorithm used for the retrievals (SFIT4 version 9.4.4 [*Rinsland et al*., 1998]) is designed to retrieve vertical profiles of one or more gases from solar absorption FTS spectra. The forward model comprises 48 layers with density-weighted effective temperatures and pressures generated by refractive ray tracing through an atmospheric path given the solar zenith angle (at the time of measurement) and the location and altitude of the spectrometer. The forward model includes a full description of the instrument lineshape, instrument distortion, and field of view. The spectroscopic parameters are based on HITRAN 2012 [*Rothman et al*., 2013]. Isotopes of CO_2 are treated separately as interfering species. The forward model also accommodates interfering solar CO lines [*Hase et al*., 2006]. Since water vapor absorption is present in the spectral microwindows, it is fitted as an interfering species with an a priori profile based on National Centers for Environmental Prediction (NCEP) reanalysis. NCEP profiles of temperature and pressure are included in the retrieval. The OCS a priori mixing ratio profiles were obtained from the Whole Atmosphere Community Climate Model (WACCM) [*Marsh et al*., 2013]; profiles were adjusted based on the mean tropopause height at each site.

The inverse model uses a semiempirical implementation of optimal estimation theory [*Rodgers*, 1976]. The a priori covariance matrix is based on the 1σ variances from WACCM. The assumed signal-to-noise ratio of the spectra is 500. This combination of regularization results in ~2 degrees of freedom. The inverse model in SFIT4 actively fits all four microwindows simultaneously, along with a background slope, wavenumber shifts, and, for Wollongong spectra recorded between 2001 and 2004, a parametrized function to model the instrument line shape.

The retrieved profiles are integrated to provide partial columns. Using the convention presented in *Rodgers* [1976], the averaging kernels and degrees of freedom were used to confirm the validity of the altitude selected to separate tropospheric and stratospheric columns. Tropospheric columns were calculated from the surface to 12.5 km at Wollongong, to 10.9 km at Lauder, and to 9.2 km at Arrival Heights. Stratospheric columns comprise the OCS column concentrations above these mean tropopause levels. Typical mean (2001 to 2014) total column values for Wollongong and Lauder are 8.9×10^{15} and 8.7×10^{15} molecules/cm^2, respectively, while for Arrival Heights, the typical mean is 8.3×10^{15} molecules/cm^2 (noting that no measurements are available in winter). The mean (2001 to 2014) tropospheric and stratospheric columns for Wollongong are 7.54×10^{15} and 1.34×10^{15} molecules/cm^2, for Lauder are 7.13×10^{15} and 1.57×10^{15} molecules/cm^2, and for Arrival Heights are 6.81×10^{15} and 1.51×10^{15} molecules/cm^2.

2.2. Analysis

As the primary focus of this study is to determine trends in OCS from all three sites, OCS anomalies are calculated with respect to the 2001 to 2014 stationary part of the annual cycle, i.e., the annual cycle that is time invariant. This stationary part of the annual cycle is calculated separately for each site by applying a linear least squares regression model (including offset and trend basis functions) to the total and partial OCS column measurements. To capture the annual cycle, the offset coefficient is expanded in four Fourier pairs for Lauder and Wollongong and in two Fourier pairs for Arrival Heights as the absence of measurements in polar darkness hampers the resolution of the seasonal cycle in OCS. Using a regression model to determine the annual cycle in OCS columns rather than calculating it from the measurements directly avoids biases due to missing data and/or extreme values in any particular month.

To estimate long-term trends in the OCS measurement series and their trend uncertainties, a linear least squares regression model was applied individually to the monthly mean OCS total, tropospheric and stratospheric column anomalies, together with their measurement uncertainties, at all three sites. As any systematic bias component of the total uncertainty of the OCS measurements does not affect the trend of the time series, only the random uncertainties are passed to the regression model. The regression model is constructed as follows:

$$\mathrm{OCS_t} = \alpha + \beta \times t_1 + \gamma \times t_2 + \delta \times t_3 + \varepsilon \times \mathrm{TropHgt_t} + R_\mathrm{t} \quad (1)$$

where $\mathrm{OCS_t}$ is the OCS column anomaly at time *t*. α to ε are the regression model fit coefficients calculated using a multivariate least squares regression approach [*Moore and McCabe*, 2003].

The OCS total, tropospheric and stratospheric column measurements, above all three sites show time-varying linear trends with two discernible inflection points. While the long-term linear trend could be estimated by applying a typical trend regression model [*Bodeker and Kremser*, 2015], the inflection points would not be appropriately accounted for. Therefore, the regression model is constructed to allow for different trends in three different periods separated by two inflection points, while ensuring that the regression fit is piecewise continuous. t_1 is the number of months after January 2001, and its associated fit coefficient (β) then represents the trend over the period to the first inflection point. t_2 is the number of months after the first inflection point and set to zero beforehand; its associated fit coefficient (γ) represents the change in trend, with respect to β, after the first inflection point. Similarly, t_3 is the number of months after the second inflection point, and its associated fit coefficient (δ) represents the change in trend with respect to γ. While the choice of the number, and timing, of the inflection points is somewhat arbitrary, the regression model can be used to guide the optimal number of inflection points, as well as their timing. Including two inflection points in the regression model resulted in the smallest sum of the squares of the residuals but avoiding overfitting. To estimate the optimal timing of the inflection points, a wide range of combinations of the timing of the inflection points, constrained by visual assessment of realistic values, was explored using the regression model to find the minimum of the sum of the squares of the residuals.

To account for the seasonality in the trend fit coefficients, these coefficients were expanded in Fourier series [*Bodeker and Kremser*, 2015], e.g., the coefficients β, γ, and δ are expanded in one Fourier pair as follows:

$$\beta = \beta_0 + \beta_1 \times \sin(2\pi M/12) + \beta_1 \times \cos(2\pi M/12) \quad (2)$$

where *M* is the month number.

The potential influence of the seasonal variation in tropopause heights is accounted for by including monthly mean tropopause heights, obtained from NCEP (National Centers for Environmental Prediction) Climate Forecast System Reanalyses, as a basis function in the regression model ($\mathrm{TropHgt_t}$). As potential trends in tropopause heights could alias into trends in OCS columns, the contribution of the trend in tropospheric heights to the trend in OCS columns was determined, and the results indicate that any contribution is small, less than 0.5% for Lauder, less than 1% for Wollongong, and less than 3% for Arrival Heights. Furthermore, to ensure that any trend in OCS is assigned exclusively to the trend basis functions, the tropopause height time series (TropHgt in equation (1)) were detrended before being used in the regression model.

R_t is the residual, i.e., that part of the signal that cannot be described by the regression model and is calculated by subtracting the model fit from the measurements. The uncertainties on trend coefficients were obtained by applying a bootstrap method [*Efron and Tibshirani*, 1986], generating 10,000 trend values

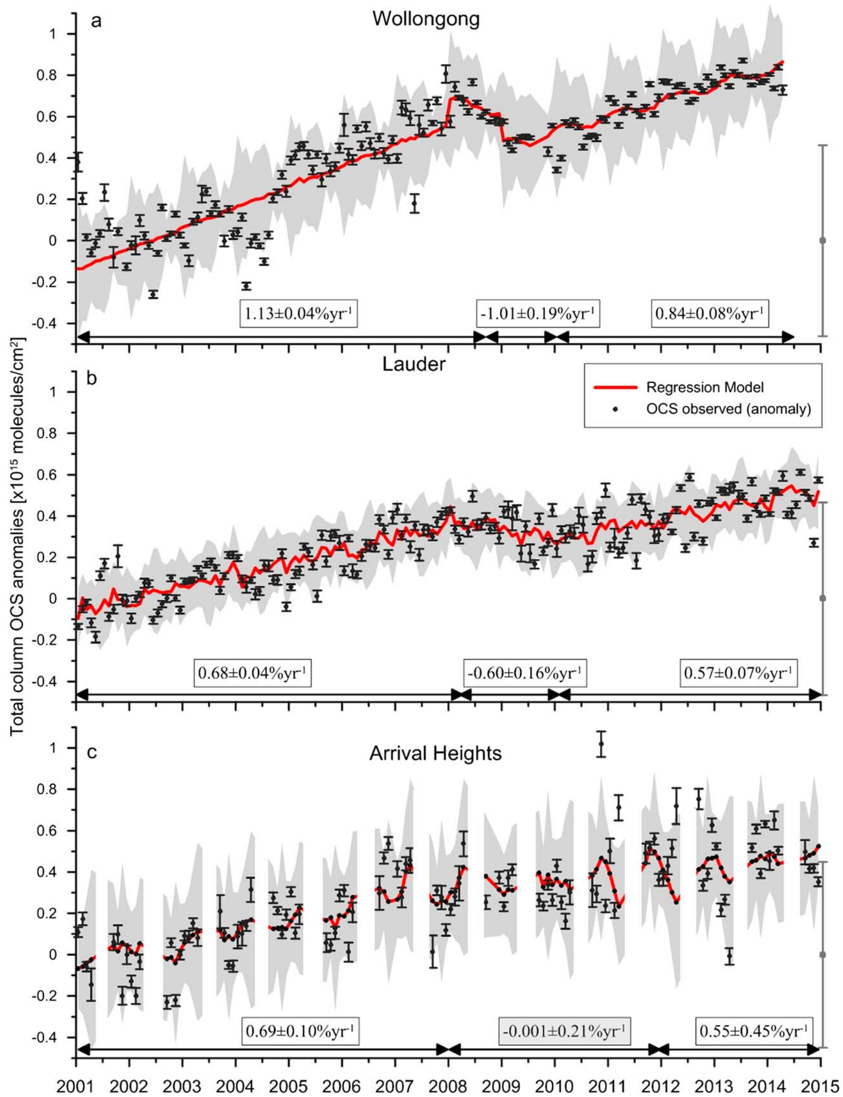

Figure 1. Monthly mean total column OCS anomalies above (a) Wollongong, (b) Lauder, and (c) Arrival Heights. OCS anomalies (black dots) are shown together with their random uncertainties (vertical error bar). The indicative total uncertainty (random + systematic) on the measurements is shown on the far right of each panel, centered on the zero line (~5%). The red line shows the regression model fit and its 2σ uncertainty (grey shading). Derived trends that are statistically significantly different from zero at the 1σ level are listed in white boxes; statistically insignificant trends are listed in grey boxes.

individually for total and partial columns. The standard deviation of those 10,000 values was then calculated to obtain the uncertainties on the trend values.

3. Results and Discussion

The monthly mean total column OCS anomalies, together with the regression model fit, are shown in Figure 1. Percentage values throughout this paper (including those for tropospheric and stratospheric columns) are with respect to the mean total column OCS above each site from 2001 to 2014. A positive trend in total column OCS is apparent at all three sites. Above Wollongong and Lauder, the strongest trend in OCS is observed from 2001 to mid-2008, followed by a ~1.5 year period of decreasing OCS and then weaker positive trends until the end of 2014. In all three periods, at both Lauder and Wollongong, derived trends are statistically significantly different from zero at the 2σ level (hereafter, simply referred to as statistically significant). Of the three sites, Wollongong shows the strongest positive trends in OCS at 1.13 ± 0.04%/yr (1σ uncertainties are quoted hereafter) for the first 7.5 years and 0.84 ± 0.08%/yr for the last 4.5 years.

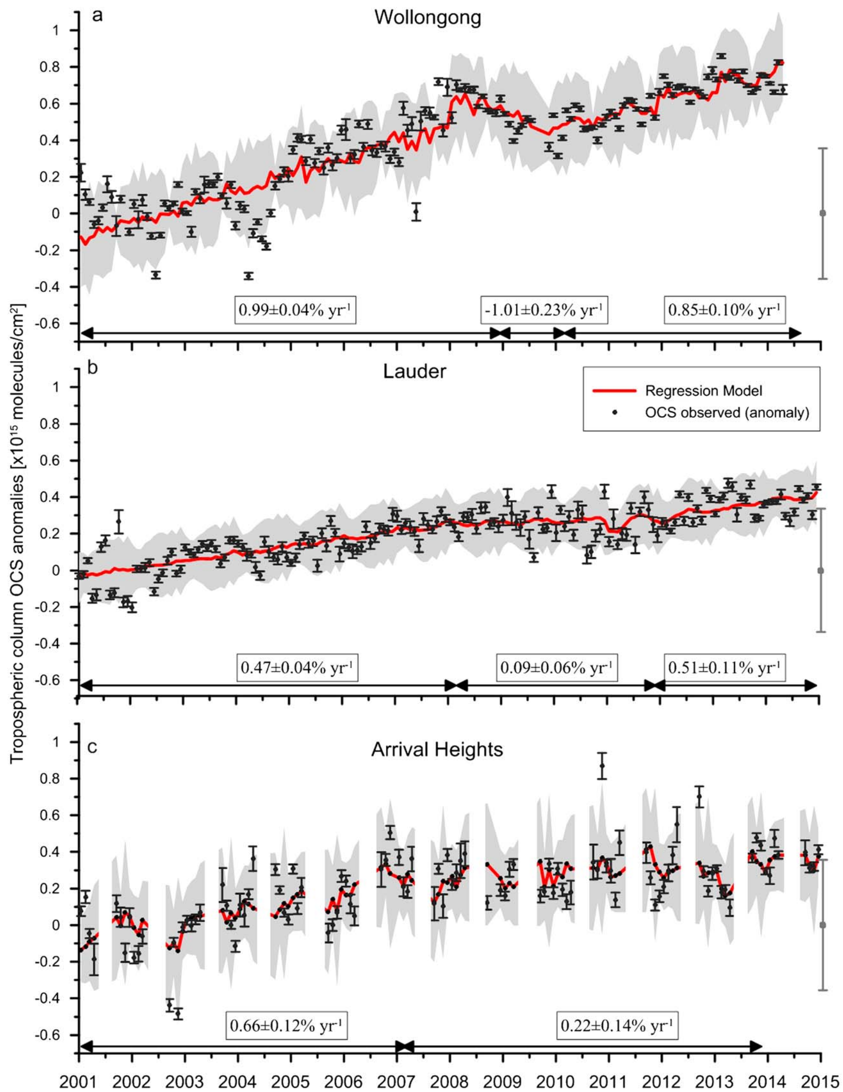

Figure 2. As in Figure 1 but for tropospheric OCS columns. The total uncertainty on the tropospheric columns is ~4.7% for all sites.

Furthermore, the reversal in the OCS trend from 2008 to the end of 2009 is most pronounced above Wollongong. Similarly, from the second quarter of 2008 to the beginning of 2010, the trend in total column OCS above Lauder changes sign, and OCS decreases by -0.60 ± 0.16%/yr. The period from 2001 to 2008, during which OCS increases above Arrival Heights, is followed by ~4 years of no discernible trend (Figure 1). During the last 3 years of the observation period, total column OCS above Arrival Heights increases at 0.55 $\pm$ 0.45%/yr. The temporal coherence of OCS trends, and the two inflection points across all three sites, has, to our knowledge, not been observed to date at any other sites in the Southern Hemisphere.

When it comes to partial columns, the short-term fluctuations in the regression model (red line in Figures 2 and 3), resulting from inclusion of the tropopause heights as a basis function (equation (1)), become more visible than looking at total OCS columns. Tropospheric OCS columns increase between 2001 and 2014 but, similar to the total columns, show time-varying trends with two inflection points, at all three sites (Figure 2). All calculated trends in tropospheric OCS columns are statistically significant, except for the trend at Lauder from 2008 to the end of 2011 and at Arrival Heights from 2007 to the end of 2013. These trends are only statistically significant at the 1σ level. The largest trend in tropospheric OCS of 0.99 ± 0.04%/yr is observed above Wollongong from 2001 to the end of 2008. While the single year of decreasing tropospheric OCS in 2009 is apparent in the Wollongong data, the positive trend weakens above Lauder from 2008 to the end of 2011 and above

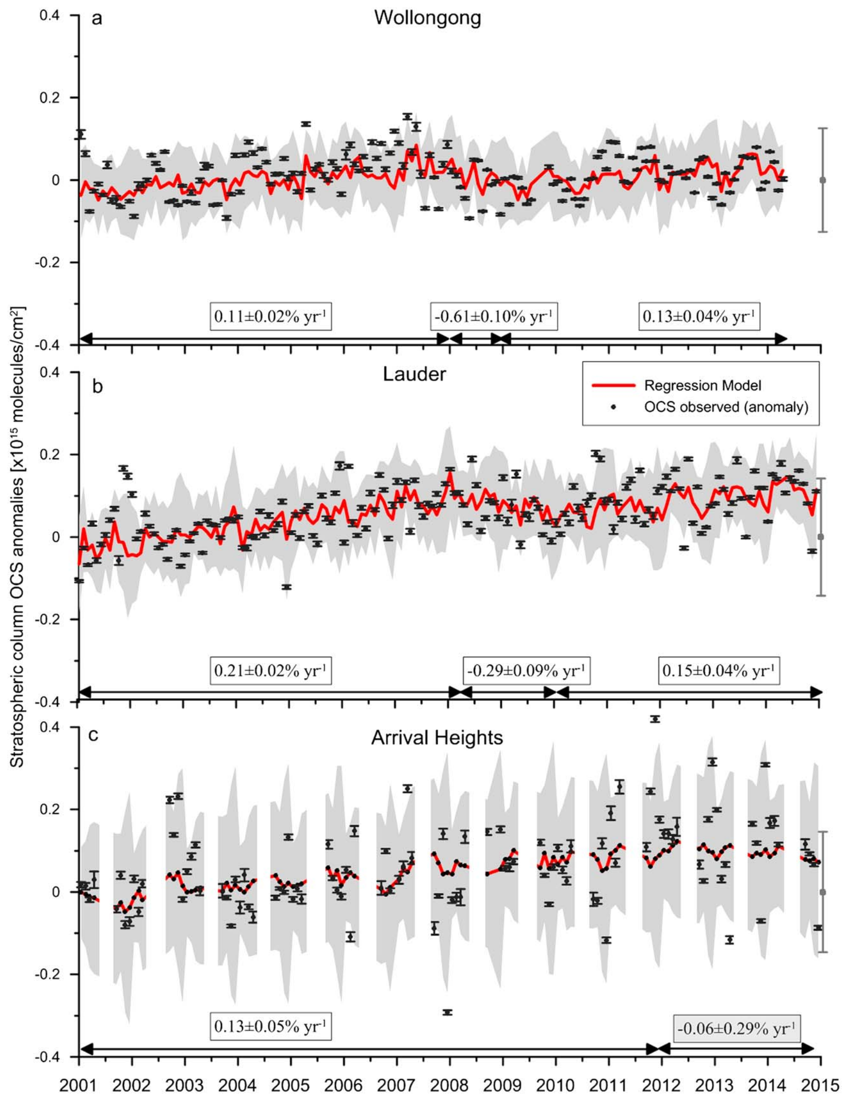

Figure 3. As in Figure 1 but for stratospheric columns. The total uncertainty on the stratospheric columns is ~9% for all sites.

Arrival Heights from 2007 to the end of 2013. Toward the end of the observation period, positive trends are observed above both Wollongong and Lauder with the Wollongong tropospheric OCS trend initiating two years earlier than at Lauder and at a greater rate. There are insufficient data after 2013 to derive a robust trend above Arrival Heights during this period, and therefore, trends over this short period are not considered.

Stratospheric OCS column anomalies above Wollongong and Lauder show similar trend structure to that observed in tropospheric and total column anomalies (Figure 3). However, unlike the tropospheric and total column anomalies where trends were strongest at Wollongong, trends in stratospheric anomalies are strongest at Lauder. Negative trends in stratospheric OCS start a few months later above Lauder compared to Wollongong and last about a year longer than at Wollongong. Both sites show a positive trend in stratospheric OCS of similar magnitude thereafter. Trends in stratospheric OCS at Lauder and Wollongong are statistically significant. Above Arrival Heights, the magnitude of the positive trend in stratospheric OCS from 2001 to the end of 2011 is comparable to the trend observed above Wollongong and weaker than observed at Lauder. The positive trend ceases toward the end of the observation period, and the trend thereafter is not statistically significant.

When examining overall trends using a regression model containing a single trend basis function, total column OCS anomalies above all three sites show clear positive trends over the full period that are statistically significant. Examination of overall trends disaggregated between the troposphere and stratosphere (as was done for the piecewise trends above) indicates that the overall trends in total column OCS are driven mainly by changes in the troposphere. The overall trend in total column OCS above Wollongong is 0.73 ± 0.03%/yr with a troposphere/stratosphere disaggregation of 94% to 6%. The overall trends in total column OCS above Lauder and Arrival Heights are very similar, showing an increase of 0.43 ± 0.02%/yr and 0.45 ± 0.05%/yr, respectively. The tropospheric/stratospheric contribution is 76% to 24% for Lauder and 82% to18% for Arrival Heights. The overall positive trend in OCS suggests that OCS sources and sinks are in imbalance. This conclusion differs from the conclusion that would be derived from previous OCS observations that do not show any trend, e.g., from flask measurements over the period 2000 to 2006 [*Montzka et al*., 2007].

The flask measurements presented in *Montzka et al*. [2007] were recently updated (http://www.esrl.noaa.gov/gmd/hats/gases/OCS.html). A detailed trend analysis of these updated flask measurements has not been published to date. A very preliminary analysis of these raw flask measurements suggests, that OCS concentrations obtained from measurement sites in the Southern Hemisphere, e.g., flask measurements obtained at Cape Grim (Australia) and Samoa (Pacific), show a small positive trend from 2010 onward. In addition, flask measurements obtained at Cape Grim show a slight decrease in OCS between 2007 and 2009. These results show that the flask measurements are broadly consistent with the FTS column data presented here. Because of the longevity of OCS, a longer-lasting trend would be expected to express itself in both in situ measurements at any station in the troposphere and FTS measurements of the whole column. However, because in situ flask measurements and tropospheric columns will be affected by transport processes in a different way, any quantitative conclusion and detailed comparison of the flask with FTS measurements are only possible via a detailed transport model which is beyond the scope of this paper.

4. Conclusion

The positive trends in OCS described above suggest that either (i) tropospheric OCS sources have increased, (ii) an additional unknown source of OCS exists (most likely of anthropogenic origin), (iii) tropospheric OCS sinks have decreased, (iv) the speed of the stratospheric circulation that transports OCS from the tropics to the middle and high latitudes has increased, or (v) the flux of OCS entering the stratosphere in the tropics has increased. An increase in OCS flux to the stratosphere could result from increased surface OCS emissions due to increases in rayon production in China over the last decade [*Campbell et al*., 2015] and subsequent transport to the stratosphere via the Asian Monsoon [*Randel et al*., 2010]. The temporal coherence of the changes in the trends across the three widely distributed sites is consistent with OCS's long lifetime in the troposphere. However, the temporal coherence of the trends may also indicate that their cause is hemispheric in scale rather than local in scale. That said, the fact that the tropospheric trend is greater than the stratospheric trend, which is the opposite of what would be expected from a change driven by large-scale dynamics such as the Brewer-Dobson circulation, detracts from the inference that the cause is hemispheric in scale. Longer OCS measurement series at globally distributed sites, together with targeted model studies that account for changes in the large-scale circulation and OCS transport, are required to address the new questions revealed in this study.

Acknowledgments
We would like to thank David Griffith, Clare Murphy, and Voltair Velazco at the School of Chemistry at the University of Wollongong and John Robinson at the NIWA research center at Lauder, New Zealand, Antarctica New Zealand, and science technicians at Scott Base for their tireless efforts to maintain FTS instrumentation and to conduct FTS measurements of OCS. Stefanie Kremser would like to thank the Royal Society of New Zealand for supporting this research through the Marsden Fast-Start Fund. The FTS measurements at Lauder and Arrival Heights are conducted as part of NIWA's government-funded, core research. The measurement program and NDACC site at Wollongong has been supported by the Australian Research Council for many years, most recent by grants DP110101948 and LE0668470. Funding by the EU project StratoClim is acknowledged. This work has partially been supported by the German Research council (Deutsche Forschungsgemeinschaft, DFG), grant PA 1714/6-1. Requests for data used in this paper can be directed to Stefanie Kremser (stefanie@bodekerscientific.com).

References

Berry, J., et al. (2013), A coupled model of the global cycles of carbonyl sulfide and CO_2: A possible new window on the carbon cycle, *J. Geophys. Res. Biogeosci.*, *118*, 842–852, doi:10.1002/jgrg.20068.

Blake, N. J., et al. (2004), Carbonyl sulfide and carbon disulfide: Large-scale distributions over the western Pacific and emissions from Asia during TRACE-P, *J. Geophys. Res.*, *109*, D15S05, doi:10.1029/2003JD004259.

Bodeker, G. E., and S. Kremser (2015), Techniques for analyses of trends in GRUAN data, *Atmos. Meas. Tech.*, *8*, 1673–1684, doi:10.5194/amt-8-1673-2015.

Brühl, C., J. Lelieveld, P. J. Crutzen, and H. Tost (2012), The role of carbonyl sulphide as a source of stratospheric sulphate aerosol and its impact on climate, *Atmos. Chem. Phys.*, *12*, 1239–1253.

Campbell, J. E., et al. (2008), Photosynthetic control of atmospheric carbonyl sulfide during the growing season, *Science*, *322*, 1085–1088.

Campbell, J. E., M. E. Whelan, U. Seibt, S. J. Smith, J. A. Berry, and T. W. Hilton (2015), Atmospheric carbonyl sulfide sources from anthropogenic activity: Implications for carbon cycle constraints, *Geophys. Res. Lett.*, *42*, 3004–3010, doi:10.1002/2015GL063445.

Chin, M., and D. D. Davis (1995), A reanalysis of carbonyl sulfide as a source of stratospheric background sulfur aerosol, *J. Geophys. Res.*, *1000*(D5), 8993–9005, doi:10.1029/95JD00275.

Coffey, M. T., and J. W. Hannigan (2010), The temporal trend of stratospheric carbonyl sulfide, *J. Atmos. Chem.*, *67*, 61–70, doi:10.1007/s10874-011-9203-4.

Crutzen, P. J. (1976), The possible importance of CSO for the sulfate layer of the stratosphere, *Geophys. Res. Lett.*, *3*, 73–76, doi:10.1029/GL003i002p00073.

Efron, B., and R. Tibshirani (1986), Bootstrap methods for standard errors, confidence intervals, and other measures of statistical accuracy, *Stat. Sci.*, *1*(1), 54–77.

Griffith, D. W. T., N. B. Jones, and W. A. Matthews (1998), Interhemispheric ratio and annual cycle of carbonyl sulfide (OCS) total column from ground-based solar FTIR spectra, *J. Geophys. Res.*, *103*(D7), 8447–8454, doi:10.1029/97JD03462.

Hase, F., P. Demoulin, A. J. Sauval, G. C. Toon, P. F. Bernath, A. Goldman, J. W. Hannigan, and C. P. Rinsland (2006), An empirical line-by-line model for the infrared solar transmittance spectrum from 700 to 5000 cm^{-1}, *J. Quant. Spectros. Radiat. Transfer*, *102*, 450–463.

Hofmann, D. J., and T. Deshler (1990), Balloonborne measurements of polar stratospheric clouds and ozone at −93°C in the Arctic in February 1990, *Geophys. Res. Lett.*, *17*(12), 2185–2188, doi:10.1029/GL017i012p02185.

Hofmann, D., J. Barnes, M. O'Neill, M. Trudeau, and R. Neely (2009), Increase in background stratospheric aerosol observed with lidar at Mauna Loa Observatory and Boulder, Colorado, *Geophys. Res. Lett.*, *36*, L15808, doi:10.1029/12009GL039008.

Jones, N. B., K. Riedel, W. Allan, S. Wood, P. I. Palmer, K. Chance, and J. Notholt (2009), Long-term tropospheric formaldehyde concentrations deduced from ground-based Fourier transform solar infrared measurements, *Atmos. Chem. Phys.*, *9*, 7131–7142.

Kettle, A. J., U. Kuhn, M. von Hobe, J. Kesselmeier, and M. O. Andreae (2002), Global budget of atmospheric carbonyl sulfide: Temporal and spatial variations of the dominant sources and sinks, *J. Geophys. Res.*, *107*(D22), 4658, doi:10.1029/2002JD002187.

Kohlhepp, R., et al. (2012), Observed and simulated time evolution of HCl, $ClONO_2$, and HF total column abundances, *Atmos. Chem. Phys.*, *12*, 3527–3556.

Kuai, L., J. Worden, S. S. Kulawik, S. A. Montzka, and J. Liu (2014), Characterization of Aura TES carbonyl sulfide retrievals over ocean, *Atmos. Meas. Tech.*, *7*, 163–172, doi:10.5194/amt-7-163-2014.

Marsh, D. R., M. J. Mills, D. E. Kinnison, J.-F. Lamarque, N. Calvo, and L. M. Polvani (2013), Climate change from 1850 to 2005 simulated in CESM1(WACCM), *J. Clim.*, *26*(19), 7372–7391.

Montzka, S. A., P. Calvert, B. D. Hall, J. W. Elkins, T. J. Conway, P. P. Tans, and C. Sweeney (2007), On the global distribution, seasonality, and budget of atmospheric carbonyl sulfide (COS) and some similarities to CO_2, *J. Geophys. Res.*, *112*, D09302, doi:10.1029/2006JD007665.

Moore, D. S., and G. P. McCabe (2003), *Introduction to the Practice of Statistics*, W.H. Freeman and Company, New York.

Myhre, G., T. F. Berglen, C. E. L. Myhre, and I. S. A. Isaksen (2004), The radiative effect of the anthropogenic influence on the stratospheric sulfate aerosol layer, *Tellus*, *56*(B), 294–299.

Paton-Walsh, C., N. Jones, S. Wilson, A. Meier, N. Deutscher, D. Griffith, R. Mitchell, and S. Campbell (2004), Trace gas emissions from biomass burning inferred from aerosol optical depth, *Geophys. Res. Lett.*, *31*, L05116, doi:10.1029/2003GL018973.

Pitari, G., E. Mancini, V. Rizi, and D. Shindell (2002), Impact of future climate change and emission changes on stratospheric aerosols and ozone, *J. Atmos. Sci.*, *59*, 414–440.

Randel, W. J., M. Park, L. Emmons, D. Kinnison, P. Bernath, K. A. Walker, C. Boone, and H. Pumphrey (2010), Asian monsoon transport of pollution to the stratosphere, *Science*, *328*, 611–613.

Rinsland, C. P., et al. (1998), Northern and southern hemisphere ground-based infrared spectroscopic measurements of tropospheric carbon monoxide and ethane, *J. Geophys. Res.*, *103*(D21), 28,197–28,217, doi:10.1029/98JD02515.

Rinsland, C. P., L. Chiou, E. Mahieu, R. Zander, C. D. Boone, and P. F. Bernath (2008), Measurements of long-term changes in atmospheric OCS (carbonyl sulfide) from infrared solar observations, *J. Quant. Spectros. Radiat. Transfer*, *109*, 2679–2686.

Rodgers, C. D. (1976), Retrieval of atmospheric temperature and composition from remote measurements of thermal radiation, *Rev. Geophys. Space Phys.*, *14*(4), 609–624.

Rothman, L. S., et al. (2013), The HITRAN2012 molecular spectroscopic database, *J. Quant. Spectros. Radiat. Transfer*, *130*, 4–50.

Sandoval-Soto, L., M. Stanimirov, M. von Hobe, V. Schmitt, J. Valdes, A. Wild, and J. Kesselmeier (2005), Global uptake of carbonyl sulfide (COS) by terrestrial vegetation: Estimates corrected by deposition velocities normalized to the uptake of carbon dioxide (CO_2), *Biogeosciences*, *2*(2), 125–132.

Sheng, J.-X., D. K. Weisenstein, B.-P. Luo, E. Rozanov, A. Stenke, J. Anet, H. Bingemer, and T. Peter (2015), Global atmospheric sulfur budget under volcanically quiescent conditions: Aerosol-chemistry-climate model predictions and validation, *J. Geophys. Res. Atmos.*, *120*, 256–276, doi:10.1002/2014JD021985.

Sturges, W. T., S. A. Penkett, J.-M. Barnola, J. Chappellaz, E. Atlas, and V. Stroud (2001), A long-term record of carbonyl sulfide (COS) in two hemispheres from firn air measurements, *Geophys. Res. Lett.*, *28*(21), 4095–4098, doi:10.1029/2001GL013958.

Suntharalingam, P., A. J. Kettle, S. M. Montzka, and D. J. Jacob (2008), Global 3-D model analysis of the seasonal cycle of atmospheric carbonyl sulfide: Implications for terrestrial vegetation uptake, *Geophys. Res. Lett.*, *35*, L19801, doi:10.1029/2008GL034332.

Vernier, J.-P., et al. (2011), Major influence of tropical volcanic eruptions on the stratospheric aerosol layer during the last decade, *Geophys. Res. Lett.*, *38*, L12807, doi:10.1029/2011GL047563.

Watts, S. F. (2000), The mass budgets of carbonyl sulfide, dimethyl sulfide, carbon disulfide and hydrogen sulfide, *Atmos. Environ.*, *34*(5), 761–779.

Wood, S. W., et al. (2002), Validation of version 5.20 ILAS HNO_3,CH_4 ,N_2O, O_3, and NO_2 using ground-based measurements at Arrival Heights and Kiruna, *J. Geophys. Res.*, *107*(D24), 8208, doi:10.1029/2001JD000581.

Zeng, G., S. W. Wood, O. Morgenstern, N. B. Jones, J. Robinson, and D. Smale (2012), Trends and variations in CO, C_2H_6, and HCN in the Southern Hemisphere point to the declining anthropogenic emissions of CO and C_2H_6, *Atmos. Chem. Phys.*, *12*, 7543–7555, doi:10.5194/acp-12-7543-2012.